ACS APPLIED MATERIALS & INTERFACES

Research Article

www.acsami.org

Enhanced Adhesion over Aluminum Solid Substrates by Controlled Atmospheric Plasma Deposition of Amine-Rich Primers

Julien Petersen,[†,‡] Thierry Fouquet,[†] Marc Michel,[†] Valérie Toniazzo,[†] Aziz Dinia,[‡] David Ruch,[†] and João A. S. Bomfim*[,†]

[†]Advanced Materials & Structures, Centre de Recherche Public Henri Tudor, Rue de Luxembourg 66, L4221 Esch-sur-Alzette, Luxembourg, and

[‡]Institut de Physique et Chimie des Matériaux de Strasbourg, (IPCMS-CNRS) UMR 7504, Université de Strasbourg, 23 rue du Lœss, BP 43, 67034 Strasbourg Cedex 2, France

S *Supporting Information*

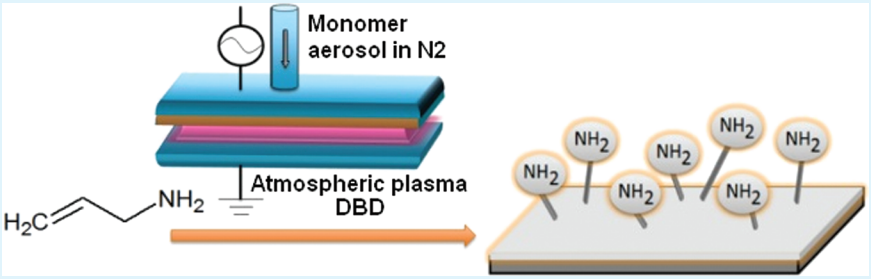

ABSTRACT: Controlled chemical modification of aluminum surface is carried by atmospheric plasma polymerization of allylamine. The amine-rich coatings are characterized and tested for their behavior as adhesion promoter. The adhesion strength of aluminum-epoxy assemblies is shown to increase according to primary amino group content and coating thickness, which in turn can be regulated by plasma power parameters, allowing tailoring the coating chemical properties. The increase in adherence can be correlated to the total and primary amino group contents in the film, indicating covalent bonding of epoxy groups to the primer as the basis of the mechanical improvement.

KEYWORDS: *adhesion, atmospheric plasma, surface modification, aluminum bonding, plasma polymerization, amine primers*

INTRODUCTION

Adhesion phenomena are mostly interfacial and the work of adhesion between two substrates largely depends on the chemical affinities of the different surfaces. Therefore, controlling the surface state of the adherends and introducing chemical groups of complementary polarity (as in Lewis acid−base chemistry) or reactivity (electrophilic or nucleophilic characters) is known to increase the adhesion strength.[1] Indeed, surface pretreatment is a key factor for adhesive bonding operations for both composite materials and structures.

A number of procedures are currently available, from wet to dry techniques.[2] The deposition of organic coatings by means of cold plasma[3−10] is a promising technique that yields stable films with tunable chemical functionality.[11] Additionally, atmospheric plasma treatment, unlike vacuum methods, allows continuous operation for in-line systems and an easier up scaling, and by using aerosolized precursors, the monomer fragmentation is reduced and the deposition rate is not limited by the vapor pressure of the organic monomers.[12−15] There are essentially two different plasma treatments for surface modification in adhesion applications: (i) air/oxygen plasma activation of the surface[16−19] and (ii) plasma polymerization for the deposition of organic or hybrid coatings.[20−25] Whereas in the first case, the increase in adhesion performance is mostly due to the removal of contamination layers, such as greases and carbonaceous matter,[16] and the subsequent facilitation of access to active sites, the second strategy deals with more extensive surface modification, in a similar way to adhesion promoters and primers.[1,26−33]

Although atmospheric plasma still present some drawbacks, mostly related to power consumption and the gas flow needed, some recent technical developments are tackling these problems through plasma-jet and plasma-curtain geometries, as well as gas recycling.[34] Moreover, given the flexibility of atmospheric plasma coating deposition, it has already attracted a number of industries to explore this technology. For instance, automotive suppliers use atmospheric plasma deposited primers to increase adhesion and aging resistance of bonded components,[35] whereas packaging industries are investigating atmospheric plasma coatings to replace conventional corona treatment for activating polyolefin surfaces.[36]

Received: December 2, 2011
Accepted: January 25, 2012
Published: January 25, 2012

Scheme 1. Atmospheric Plasma Polymerization of Allylamine

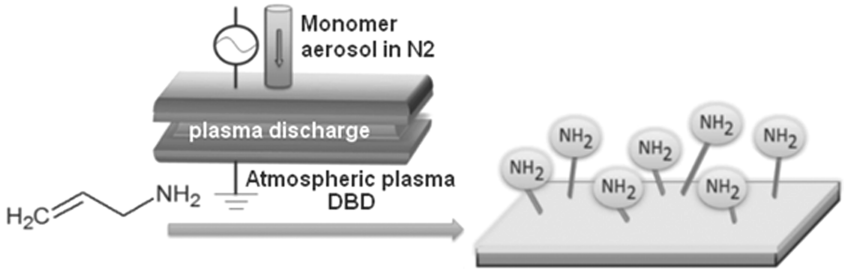

The controlled incorporation of functional groups is of particular interest for fine-tuning the adherend-adhesive interaction through tailor-made surface treatments. In this frame, amine-rich surfaces are an attractive approach to improve the adhesion properties. Several authors highlighted that deposition of amino groups lead to reactive surfaces. Different ways have been used to deposit nitrogen functional groups such as plasma polymerization at low pressure of *N*-containing monomer. Several nitrogen containing precursors have been used to deposit NH_2 groups, such as allylamine,[37,38] n-butylamine,[39] ethylenediamine,[40] or propylamine.[41] Results clearly showed that the content and the nature of amino groups could be tune by plasma parameters and specially the power injected in the plasma. Denis et al. have highlighted that the plasma polymerization is due to the dissociation of chemical bond by plasma species and to the chemical reaction such as hydrogen addition.[42] On other hand, water-based "layer-by-layer" process is also a versatile method for fine-tuning the surface with functional groups.[43−45] Indeed, absorption of polyelectrolyte species on substrate leads to the alternation of physicochemical properties of the surface. Nevertheless, these kinds of process are limited by deposition time, the size or the shape of substrate, limited to the batch process or using solvent. Another study proposed to functionalize surfaces, mostly for biomedical applications, by plasma polymerization at atmospheric pressure of mixtures containing hydrocarbon precursors and gases such as N_2 or NH_3;[46] although a high level of nitrogen incorporation has been achieved, the final concentration of primary amine groups was fairly low.

Aluminum-epoxy adhesive joints, used in several technological applications, such as aerospace composites, normally employ two-part epoxy resins with polyamine hardeners. Indeed, it is well established that after adhesive application there is a complex process of interphase formation including an amine-to-aluminum adsorption step prior to adhesive curing[47] and that, after curing, this interphase is in great part responsible for the epoxy-aluminum strong affinity.[48]

In this work, we prepared a series of amine-rich organic coatings by atmospheric plasma polymerization of allylamine monomers (Scheme 1) and characterized the resulting films by mass (MS), X-ray photoelectron (XPS), and Fourier transformed infrared (FTIR) spectroscopies as well as chemical derivatization. To the best of our knowledge, this report is the first application of an atmospheric plasma-deposited polyamine coating for improved adhesion of aluminum adherends and the first application of poly(allylamine) (pPAAm) for structural bonding. The adhesion properties of the coatings were determined by pull-off tests and displayed higher substrate-adhesive adherence strength than the reference uncoated substrate.

EXPERIMENTAL DETAILS

Allylamine and DER332 (BADGE: bisphenol A diglycidyl ether) were purchased from Sigma-Aldrich and used as received. Aluminum 1050 substrates from Alu-Co2 (Luxembourg) were degreased and cleaned by scrubbing with acetone prior to the deposition process. Plasma polymer allylamine (pPAAm) films were deposited using a semi-dynamic DBD reactor at open atmosphere described elsewhere.[49]

The substrates (50 cm^2) were positioned at the bottom electrode and Yasuda's parameters were varied during this work. The precursor was atomized at different flow rates and injected into the N_2 carrier gas before entering the plasma zone through a slit between the two top electrodes. The deposition by plasma discharge was carried out at atmospheric pressure and at room temperature. During the experiment, the top electrode block moved over the sample at a constant speed (4 m min^{-1}); sample thickness was controlled by the number of passes. Electrical discharge was varied during each deposition ranging from 21 kV to 30 kV, which corresponded to a power density over the electrodes in the range of 0.6 − 1.6 W cm^{-2}.

Mass deposition rates were obtained by weighing glass slides before and after deposition with a microbalance. The chemical composition of the coatings was evaluated by plasma polymer deposited on KBr substrates, analyzed by FT-IR spectroscopy in transmission mode with a Bruker Optics Tensor 27 spectrometer. XPS analyses were performed with a system described elsewhere.[49] The film thickness was determined by means of single wavelength ellipsometry (PZ 2000, Jobin Yvon, France) at an angle of incidence of 70°. The plasma polymerized films were considered to be homogeneous with constant refractive index of 1.5 at 632.8 nm. The thickness values were calculated by adjusting a Fresnel model to the measured ψ and Δ values.

The surface density of amino groups in the pPAAm film was determined by chemical derivatization and UV−visible absorption spectrometry. The derivatization methods have been used as described previously.[50] First, all accessible amine groups have been determined with derivatization by bromophenol blue (BPB). After plasma treatments, films have been dipped during 30 min in BPB in DMF solution at 0.05 M. After completion samples were rinsed with absolute ethanol then dried under N_2 flow. Finally, the attached BPB molecules are extracted with piperidine/DMF and quantified at 626 nm by spectrophotometry. Afterward, 4-nitrobenzaldhehyde and *p*-nitro-benzoyl chloride were chosen to determine respectively primary and secondary amino content at the surface of plasma polymer film. Films deposited on glass slides were treated with excess reactant in anhydrous ethanol solution during 3 h at 50 °C and under argon atmosphere. After completion, all substrates were thoroughly washed with absolute ethanol to remove excess reagent and dried in a vacuum.

The surface density of primary amino groups in the pPAAm film was also determined by derivatization methods in vapor phase.[51] After deposition, samples have been directly placed in a Schlenk-type flask, to which vacuum was applied. This flask was connected to another one containing 4-(trifluoromethyl)benzaldehyde (TFBA) which, as a vapor, was allowed to react with the pPAAm films at room temperature for 4 h, after what the system has been evacuated again for 1 h to remove unreacted TFBA. The NH_2 group has been evaluated by XPS following the specific CF_3 groups in the reactant and

estimated by the eq 1 (where [A] is the atomic concentration of A measured by XPS):

$$\%NH_2 = \frac{[NH_2]}{[N]} = \frac{[F]/3}{[N]} \quad (1)$$

High-resolution MS experiments were performed using a QStar Elite mass spectrometer (Applied Biosystems SCIEX, Canada) equipped with an ESI source operated in the positive mode. The capillary voltage was set at +5500 V and the cone voltage at +10 V. In this hybrid instrument, ions were measured using a Q-TOF mass analyzer. In MS, accurate mass measurements were performed using two reference ions from a poly(ethylene glycol) internal standard, according to a procedure described elsewhere.[52] Air was used as the nebulizing gas (10 psi), whereas nitrogen was used as the curtain gas (20 psi). Instrument control, data acquisition and data processing of all experiments were achieved using Analyst software (QS 2.0) provided by Applied Biosystems. The plasma-polymerized allylamine was first dissolved in water and further diluted using a methanol with ammonium acetate (3 mM) solution to a final 10 mg L^{-1} concentration. Sample solutions were introduced in the ionization source at a 5 μL min^{-1} flow rate using a syringe pump.

Pull-off tests were performed as described in published standards using a force-controlled DeFelsko AT-A adhesion tester at 0.2 MPa s^{-1}.[53] Adhesive bonded assemblies were prepared using standard 20 mm Al dollies and 2-part epoxy adhesive Araldite 2011 (main components: BADGE and N,N-dimethyl-diethylenetriamine). The adhesive was cured at R.T. for 36 h (according to supplier instructions) which resulted in 85% cross-linking as determined by DSC. For each measurement series a reference uncoated sample was also tested; all reference adhesion strength values are statistically identical. Fracture type was assigned after visual inspection of samples after test.

RESULTS AND DISCUSSION

Initially, the plasma-chemistry of allylamine polymerization was investigated for determining suitable process conditions for obtaining amine-rich coatings. By keeping a constant monomer mass flow rate and changing applied power between 0.6 W cm^{-2} and 1.6 W cm^{-2} we investigated the effect of the so-called "Yasuda" or W/FM parameter (where W is the electrical power absorbed by the plasma, F the flow of monomer and M its molar mass, used here in a simplified form as W/F) on the structure and the mass deposition rate (Figure 1) of the final materials.

The pPAAm mass yield rate and total NH_2 content were found to decrease with increasing applied power per molecule. Hegemann and co-workers[54] evidenced that different plasma regimes could be observed by plotting the deposition rate normalized by flow rate (R_m/F) according to the W/F parameter. The Arrhenius-type plot allow to determine an activation energy from the eq 2, where R_m is the mass rate deposition and G correspond to a geometrical factor depending of plasma reactor.

$$\frac{R_m}{F} = Ge^{-\frac{E_a}{W/F}} \quad (2)$$

The apparent energy activation represents a minimum of energy to initiate plasma polymerization. Nevertheless, this approach and especially the values of E_a and G are still a matter of discussion because they exclude parameters influencing the deposition such as the pressure or the formation of cross-linked and oligomer-like layers. In our case, for the mass deposition rate, a discontinuity is observed around F/W = 0.15 cm^3/J, indicating two different plasma film-growth mechanisms: at high powers fragmentation and dissociation are favored while at lower powers the pPAAm film is formed by radical-step growth polymerization.[42]

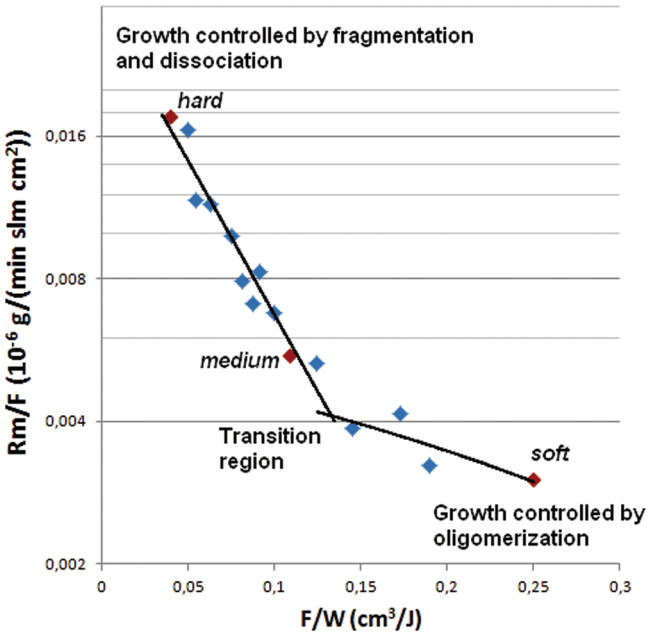

Figure 1. Mass deposition rate of pPAAm films (R_m/F) as a function of F/W parameter with indication of preparation conditions for samples described as "soft", "medium", and "hard", according to plasma power.

Likewise, FTIR investigation (Figure 2) of the deposed films indicated that N−H band at 3300 cm^{-1} decreases in intensity with increasing W/F ratio. Indeed, with increasing applied power there is also an increase of other functional groups than aliphatic amines, such as nitriles and isonitriles (C≡N peaks at 2180 and 2240 cm^{-1}) or amides and imines (broad CN and CO peak at 1620−1670 cm^{-1}). These findings are consistent with different polymerization mechanisms taking place at each film-growth conditions. At energy-intensive, "harder", conditions of high mass yields and high presence of oxidized and

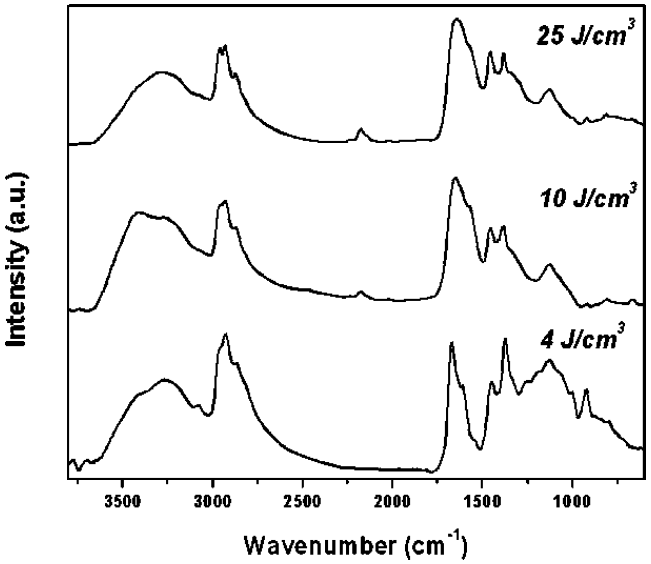

Figure 2. FTIR spectra of plasma-polymerized allylamine at different W/F parameters.

dx.doi.org/10.1021/am201699a | ACS Appl. Mater. Interfaces 2012, 4, 1072−1079

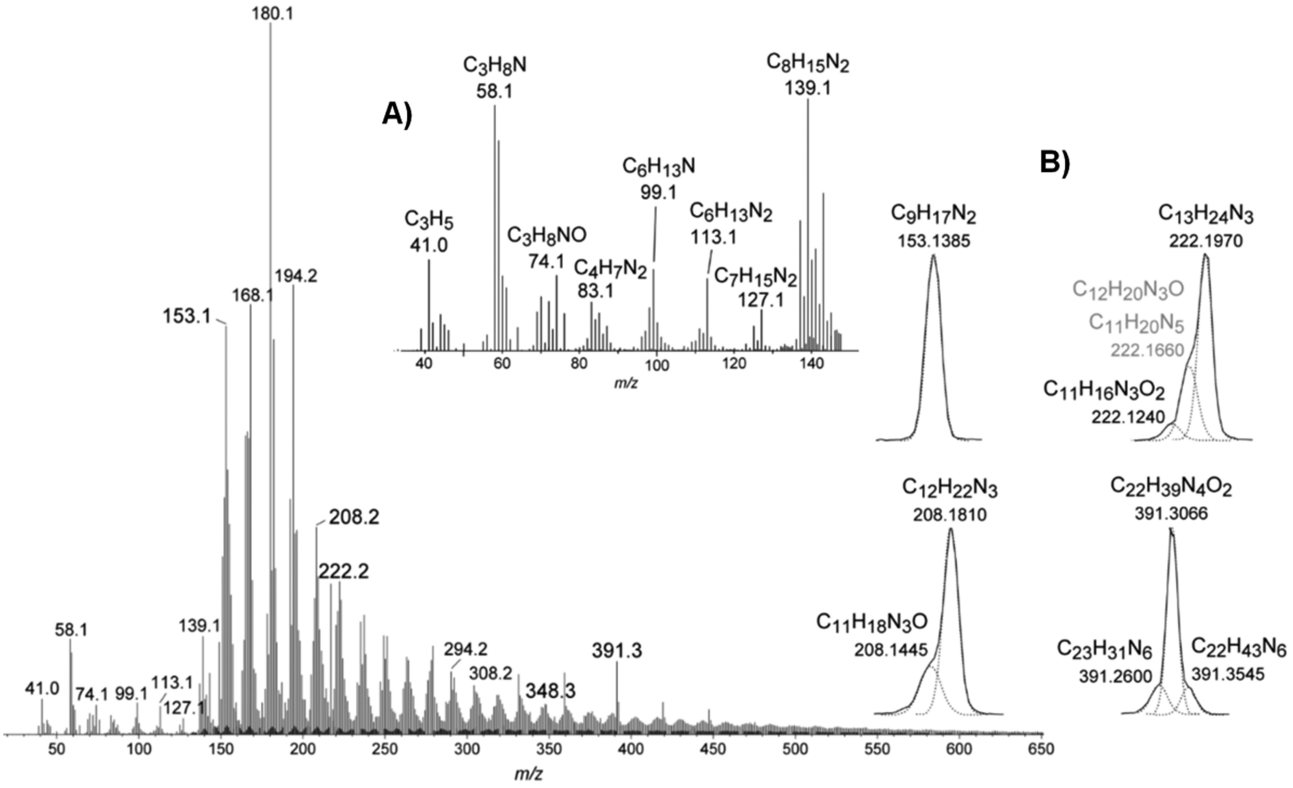

Figure 3. ESI-MS spectrum of poly(allylamine) coating; inset A, zoom on low MW species formed by fragmentation; inset B, deconvoluted peaks of quasi-isobaric species.

Table 1. XPS Analysis of pPAAm Films, Atomic Concentrations before and after TFBA Derivatization

	as-deposited			TFBA-derivate				element ratio		functional groups from C1s peak deconvolution			
W/F (J/cm^3)	C	N	O	C	N	O	F	N/C	O/C	C−C, C−H	C−N	−C−O−, −C=N−	C=O−, O=C−N−
4 (soft)	68	24.9	7.1	59.3	16.1	11.8	12.8	0.36	0.1	50	31.4	14	4.6
5.5	68.4	24.6	7	60.6	16.8	10.9	11.7	0.36	0.1	49.8	30.5	14.6	5.1
10 (medium)	69	23.9	7.1	62.4	17.3	10.6	9.7	0.34	0.1	49.1	30.2	15.4	5.3
16.6	70.6	22.3	7.1	66.6	17.6	9.3	6.5	0.32	0.1	50.5	29.2	15.2	5.1
25 (hard)	71.8	21.2	7	68	18.4	8.7	4.9	0.29	0.1	51.9	29.8	13.1	5.2

unsaturated functions is coherent with a mechanism based on allylamine fragmentation/dissociation and recombination, whereas that under "softer conditions", soft as defined previously,[14,55] is consistent with a mechanism based on radical oligomerization.

Further insight into polymer structure was gained by ESI-MS (electrospray ionization MS)[56] of water-soluble pPAAm, which exhibits a quite complex ion series pattern, from the lowest mass-to-charge ratios of m/z 30 up to m/z 650 approximately (Figure 3). On the basis of accurate mass measurements, all of these ionic species could be described as more or less unsaturated C_xH_y hydrocarbon chain (C_3H_5, m/z 41) or nitrogen-containing $C_xH_yN_z$ structures − from one (C_3H_8N at m/z 58.1) to seven nitrogen atoms ($C_{14}H_{28}N_7$ at m/z 294.2). The great variety in terms of unsaturations (DBE, double bond equivalents, from 0.5 to 12.5) could assess for both double bond preservation and cyclization mechanisms during the plasma discharge (more detailed ESI-MS results are available in the Supporting Information). Several $C_xH_yN_zO_w$ oxygenated species are also readily detected (C_3H_8NO at m/z 74.1, $C_{10}H_{16}N_3O$ at m/z 194.2 or $C_{16}H_{26}N_3O_3$ at m/z 308.2 for instance), suggesting reaction of the amine groups with residual oxygen during the deposition or afterward, upon air exposure, due to longer-lived radicals.[57] It should be noted that even though electrospray is one of the softest ionization techniques, the majority of ions detected in the very low mass range (up to m/z 130, Figure 3, inset A) are suspected to emerge from in-source dissociation reactions, as shown by the dramatic increase of their intensities and the decrease of bigger ions abundances when ionization parameters are deliberately hardened.

A closer inspection of the peak shape of some ions indicates that these signals should not be assigned to a unique ionic species, as depicted for m/z 208, m/z 222, and m/z 391 in Figure 3 (insert B). Deconvoluted signals could however be proposed based on the irregularity of the peak shapes (as compared to the unique $C_9H_{17}N_2$ signal at m/z 153.139). Two ions are thus shown to contribute to the signal at m/z 208, $C_{12}H_{22}N_3$ at m/z 208.180824 and $C_{11}H_{18}N_3O$ at m/z 208.144439, while three distinct species are detected at m/z 391, $C_{22}H_{43}N_6$ at m/z 391.354372, $C_{22}H_{39}N_4O_2$ at m/z 391.306753 and $C_{23}H_{31}N_6$ at m/z 391.260471. High-resolution MALDI-FT-ICR experiments have been further performed to assess for these deconvolutions and check for any other unresolved isobaric species. No new ion series was found, the same $C_xH_yN_zO_w$ species being detected on the same mass range and with comparable relative intensities, but some

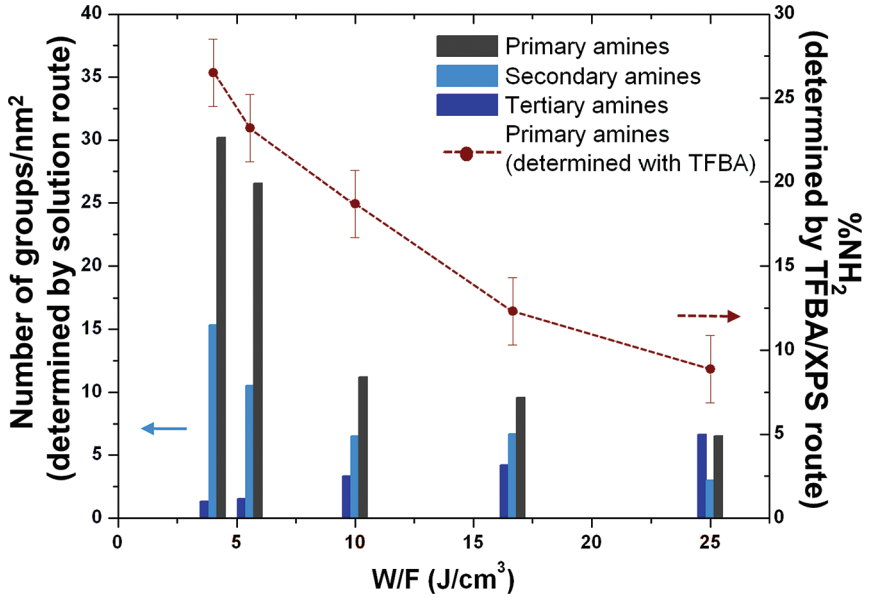

Figure 4. Amine composition and content according to *W/F* plasma parameters, as measured by solution route or TFBA/XPS route.

deconvolutions done on the ESI-MS spectrum were shown to be incomplete. As depicted in Figure 3 (insert B), the *m/z* 222 ESI-MS signal was deconvoluted into three distinct peaks at *m/z* 222.1240 ($C_{11}H_{16}N_3O_2$), *m/z* 222.1970 ($C_{13}H_{24}N_3$) and *m/z* 222.1660 (no assignment). The MALDI-FT-ICR-MS spectrum actually exhibits two isobaric species at 222.171322 ($C_{11}H_{20}N_5$) and *m/z* 222.160089 ($C_{12}H_{20}N_3O$), unresolved in the ESI-MS spectrum. Further MS info is available as Supporting Information. Overall, MS techniques confirm a nitrogen-rich coating with an oligomer composition, similar to a branched aliphatic polyamine, which can be traced back to allylamine monomers incorporating methylene fragments generated under plasma conditions.

The pPAAm coatings were further analyzed by XPS and chemical derivatization (atomic content results are presented in Table 1). The analysis performed on coatings deposited at soft or harsh (4 J/cm^3 and 25 J/cm^3 respectively) conditions indicated a marked decrease in the N/C ratio from 0.36 to 0.29 with increasing plasma power, and constant presence of about 7% O atoms. A theoretical N/C ration can be calculated for a regular poly(allylamine) from its molecular formula, which contains 1 N atom for each 3 C atoms, that is, N/C = 0,33. For the pPAAm obtained at softer conditions, the N/C ratio higher that the theoretical one can be explained by the incorporation of N-atoms in the film coming from N_2 carrier gas.[46] On the contrary, the lower N/C ratio obtained for pPAAm at harder conditions is consistent with a poly(allylamine) which underwent oxidation and, at higher power conditions, fragmentation and loss of nitrogen-containing species. As during the deposition the substrates were constantly flushed by N_2 gas, the oxidation is believed to take place after the deposition step by reaction of ambient air O_2 with reactive sites, such as remaining radicals at pPAAm surface. Deconvolution of C1s and N1s peaks provided further insight on the pPAAm coating composition, indicating noticeable concentrations of oxygenated groups such as amides or unsaturated CN bonds as in nitriles and imines (XPS results are summarized in Table 1).

The chemical derivatization technique[50] was applied to unambiguously determine the amino groups accessible to incoming reactants (assimilated to adhesive molecules) and to differentiate between primary, secondary and tertiary amines (Figure 4). As each type of amino group presents a different reactivity toward epoxy moieties, it is important to know this information to rationalize the results. Primary amines are more reactive and can bond to two different epoxy groups, while secondary amines can react with only one incoming epoxy moiety. Tertiary amines are mostly considered as catalysts for the epoxy polymerization.[1] As the derivatization studies were with wet-chemistry techniques, the plasma-coated surfaces were treated with solvents (mostly DMF and ethanol), and partial solubilization of the plasma-polymer cannot be ruled out. Therefore, the functional group speciation reflects the insoluble fraction chemical composition, which should be, in any case, the layer strongly bonded to the substrate, which also works as adhesion promoter. The solution-based chemical derivatization results were verified by the better-known vapor phase derivatization experiments,[51] which have also been performed for films obtained at each W/F ratio. Results evidenced the same tendency than the chemical derivatization, where the amount of NH_2 groups decrease when the power input per molecules increase due to an increasing of degree of fragmentation and recombination. It is, however, important to note that the reactants used in vapor phase derivatization can present side reactions over plasma-deposited films, rendering this technique nonspecific.[58]

pPAAm prepared under softer conditions were found to contain up to 30 NH_2 groups per nm^2 while at harder conditions the primary amino group surface concentration was only 6 NH_2 nm^{-2} (in agreement with FTIR observations), indicating a shift from "monomer sufficient" regime where oligomerization prevails to a "monomer deficient" one which leads to extensive fragmentation with increasing applied power. In either case, the observed NH_2 concentrations are higher than those previously reported, which is ascribed to the deposition method, employing allylamine as liquid aerosol in N_2 carrier gas.

The increased affinity between model epoxy resin BADGE and pPAAm-coated aluminum (compared to plain degreased-only aluminum) can be assessed by contact angle measurements (the comparison is shown in Figure 5). It is possible to

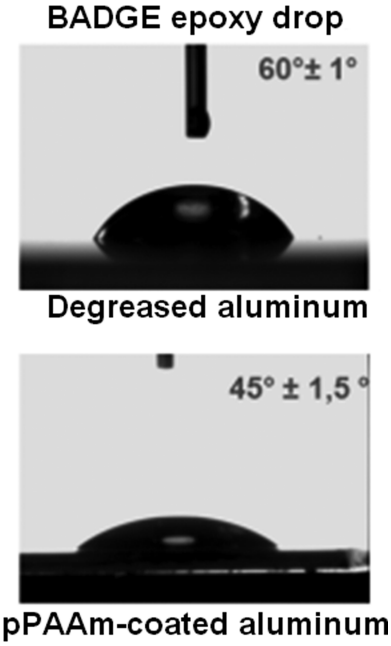

Figure 5. Contact angles for BADGE epoxy resin (bisphenol A diglycidyl ether) droplets over plain and pPAAm-coated aluminum substrates.

observe a considerable decrease in the contact angle of BADGE droplets, going from 60° for plain aluminum to about 45° for pPAAm-coated aluminum. This decrease is ascribed to the incorporation of amino groups, which favored the wetting of aluminum surface by the epoxy resin.

The application of the different pPAAm coatings as adhesion promoters for epoxy-aluminum bonded assemblies was evaluated by mechanical pull-off tests,[20] which evidenced the increase in the adhesion strength after adherend coating with reactive amino groups. The two-part epoxy adhesive Araldite 2011 was employed due to its slow room-temperature curing properties. Initially, a comparison between three sets of substrates was performed: degreased uncoated aluminum plus pPAAm-coated Al under soft and hard conditions (15 nm thick). The breaking strengths were recorded for each set (Figure 6). The results clearly indicate an increased mechanical performance for pPAAm-coated aluminum compared to uncoated one. Moreover, the pPAAm prepared at softer conditions yielded far better results than pPAAm coated at harder ones. The mode of failure, from visual inspection is of the adhesive type, between epoxy adhesive and aluminum substrate or pPAAm coating and Al substrate. These results are in agreement with the chemical composition (especially the NH_2 content) of the pPAAm layers; indeed, a higher concentration of primary amino groups leads to higher adhesion strength than a lower one, and in any case the priming of aluminum adherends with an adhesion-promoting layer leads to increased adhesion as well. A smaller adherence of allylamine coatings prepared under harder conditions could be also attributed to lower mechanical properties of this plasma polymer arising from an irregular structure from extensive fragment recombination during the plasma deposition. However, the absence of cohesive failure in the mechanical tests points mostly to a weaker interfacial adhesion.

Further insight was gained by performing pull-off adhesion tests on pPAAm coatings prepared at soft conditions but with

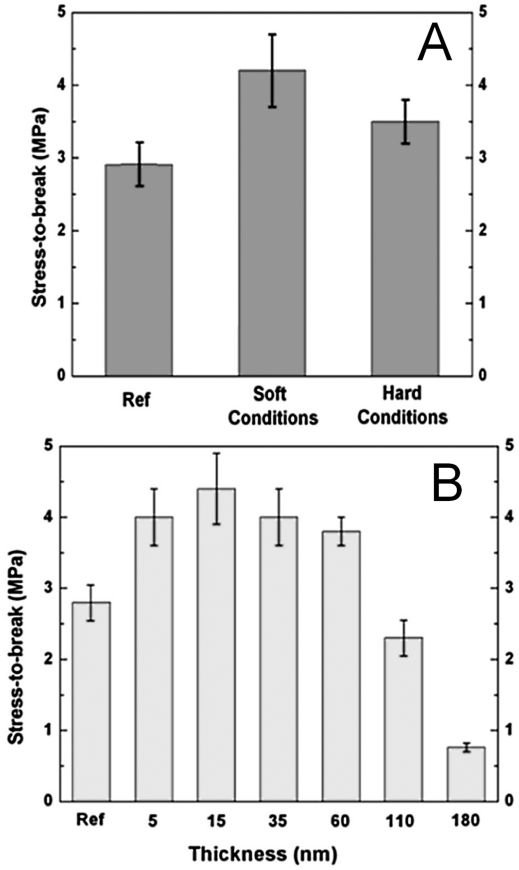

Figure 6. Adhesion strength of aluminum-epoxy assemblies with pPAAm thin coatings as adhesion promoters (A) as a function of plasma parameters and (B) as a function of coating thickness at soft conditions.

different thickness. Near-Gaussian behavior was observed, with maximum adhesion-promoting properties for 15 nm thick coatings. Adhesion promoting properties were observed for coatings between 5 and 60 nm thickness, with about 4 MPa breaking strength, but for coatings over 100 nm thick a sharp decrease in properties was observed. The fractured surfaces were inspected visually and indicate an adhesive failure in the substrate-pPAAm interface, although for coatings more than 100 nm thick there are also evidence of cohesive failure inside the pPAAm layer.

The exact role of low-molecular-weight species in the adhesion properties is still not yet clear, although these polyaminated compounds should participate in the epoxy cross-linking reaction. Indeed, it has been established that aluminum/2-part epoxy adhesive joints present a high concentration of amines in the aluminum interface due to adsorption and amine-depleted regions a little farther away from the surface. Using amine-rich substrates, which also contain soluble polyamines which participate in the adhesive cross-linking should avoid these inhomogeneities in the adhesive layer and therefore present lesser weak spots.

CONCLUSIONS

In conclusion, we demonstrated the adhesion−promotion capabilities of surface-functionalized adherends by using scalable atmospheric plasma. The key for this enhanced adhesion is the introduction of chosen reactive groups and the determination of deposition conditions for retaining the

monomer structure. For this, we investigated different deposition conditions to create poly(allylamine) coatings by atmospheric plasma polymerization, using different parameters as power output and monomer flow. The final concentration of primary amino groups was related to the W/F parameter, as harder/more energetic conditions led to increased fragmentation, whereas milder conditions yielded more regular, amine-rich coatings. These amine-rich coatings were shown to increase epoxy-aluminum affinity, as observed in contact angle measurements. By changing the deposition procedure, it was also possible to create coatings with different thickness. The amine content, which was also shown to influence wettability, and the coating thickness were finally shown to influence the adhesion promotion properties of the poly(allylamine) coatings; a correlation of primary amino group content with adhesion strength was observed. This is coherent with coating-epoxy resin condensation reaction, as well as an optimum average coating thickness of 15 nm, with adhesion strength being strongly reduced for films thicker than about 100 nm. Ongoing work deals with medium- and long-term properties of these poly(allylamine) organic coatings and the effect of temperature on their stability.

■ ASSOCIATED CONTENT

Supporting Information

MS *m/z* peak tables, FT-IR and XPS spectral data. This material is available free of charge via the Internet at http://pubs.acs.org.

■ AUTHOR INFORMATION

Corresponding Author

*E-mail: joao.bomfim@tudor.lu.

Notes

The authors declare no competing financial interest.

■ ACKNOWLEDGMENTS

The authors acknowledge the FNR, Fonds National de La Recherche of Luxembourg, and Collège Doctoral Européen de Strasbourg. Dr. Vincent Ball is also greatly acknowledged for fruitful discussions.

■ REFERENCES

(1) Petrie, E. M. In *Handbook of Adhesives and Sealants*; McGraw-Hill: New York, 2007; pp 39−57.
(2) Hyland, M. G. In *Handbook of Aluminum*; Totten, G. E., MacKenzie, D. S., Eds.; Marcel Dekker: New York, 2003; Vol. 2, pp 465−478.
(3) Heyse, P.; Dams, R.; Paulussen, S.; Houthoofd, K.; Janssen, K.; Jacobs, P. A.; Sels, B. F. *Plasma Process. Polym.* **2009**, *4*, 145−157.
(4) Bhattacharyya, D.; Yoon, W.-J.; Berger, P.-R.; Timmons, R. B. *Adv. Mater.* **2008**, *20*, 2383−2388.
(5) Desmet, T.; Morent, R.; De Geyter, N.; Leys, C.; Schacht, E.; Dubruel, E. *Biomacromolecules* **2009**, *10*, 2351−2378.
(6) Michel, M.; Bour, J.; Petersen, J.; Arnoult, C.; Ettingshausen, F.; Roth, C.; Ruch, D. *Fuel Cells* **2010**, *10*, 932−937.
(7) Gherardi, N.; Gouda, G.; Gat, E.; Ricard, A.; Massines, F. *Plasma Sources Sci. Technol.* **2000**, *9*, 340.
(8) Girard-Lauriault, P.-L.; Mwale, F.; Iordanova, M.; Demers, C.; Desjardins, P.; Wertheimer, M. R. *Plasma Process. Polym.* **2005**, *2*, 263.
(9) Teare, D. O. H.; Schofield, W. C. E.; Garrod, R. P.; Badyal, J. P. S *Langmuir* **2005**, *21*, 10818−10824.
(10) Vogelsang, A.; Ohl, A.; Foest, R.; Schröder, K.; Weltmann, K.-D. *Plasma Process. Polym.* **2011**, *8*, 77−84.
(11) Whittle, J. D.; Short, R. D.; Douglas, C. W. I.; Davis, J. *Chem. Mater.* **2000**, *12*, 2664−2671.
(12) Ward, L. J.; Schofield, W. C. E.; Badyal, J. P. S *Langmuir* **2003**, *19*, 2110−2114.
(13) Ward, L. J.; Schofield, W. C. E.; Badyal, J. P. S *Chem. Mater.* **2003**, *15*, 1466−1469.
(14) Tatoulian, M.; Arefi-Khonsari, F.; Tatoulian, L.; Amouroux, J.; Borra, J. P. *Chem. Mater.* **2006**, *18*, 5860−5863.
(15) Tatoulian, M.; Arefi-Khonsari, F.; Borra, J. P. *Plasma Process. Polym.* **2007**, *4*, 360−369.
(16) Sperandio, C.; Bardon, J.; Laachachi, A.; Aubriet, H.; Ruch, D. *Int. J. Adhesion Adhesives* **2010**, *30*, 720−728.
(17) Shenton, M. J.; Stevens, G. C. *J. Phys. D: Appl. Phys.* **2001**, *34*, 2761.
(18) Millare, B.; Thomas, M.; Ferreira, A.; Xu, H.; Holesinger, M.; Vullev, V. I. *Langmuir* **2008**, *24*, 13218−13224.
(19) Gonzalez, E. II; Hicks, R. F. *Langmuir* **2010**, *26*, 3710−3719.
(20) Petersen, J.; Bechara, R.; Bardon, J.; Fouquet, T.; Ziarelli, F.; Daheron, L.; Ball, V.; Toniazzo, V.; Michel, M.; Dinia, A.; Ruch, D. *Plasma Process. Polym.* **2011**, *8*, 895−903.
(21) Denes, F. S.; Manolache, S. *Prog. Polym. Sci.* **2004**, *29*, 815−885.
(22) Øye, G.; Roucoules, V.; Cameron, A. M.; Oates, L. J.; Cameron, N. R.; Steel, P. G.; Badyal, J. P. S; Davis, B. G.; Coe, D.; Cox, R. *Langmuir* **2002**, *18*, 8996−8999.
(23) Hu, J.; Yin, C.; Mao, H.-Q.; Tamada, K.; Knoll, W. *Adv. Funct. Mater.* **2003**, *13*, 9−24.
(24) Becker, C.; Petersen, J.; Mertz, G.; Ruch, D.; Dinia, A. *J. Phys. Chem. C* **2011**, *115*, 10675−10681.
(25) Dong, Fu, G.; Zhang, Y.; Kang, E.-T.; Neoh, K.-G. *Adv. Mater.* **2004**, *16*, 9−10.
(26) Airoudj, A.; Schrodj, G.; Vallat, M.-F.; Fioux, P.; Roucoules, V. *Int. J. Adhesion Adhesives* **2011**, *31*, 498−506.
(27) Alexander, M. R.; Whittle, J. D.; Barton, D.; Short, R. D. *J. Mater. Chem.* **2004**, *14*, 408−412.
(28) Tarducci, C.; Kindmond, E. J.; Badyal, J. P. S; Brewer, S. A.; Willis, C. *Chem. Mater.* **2000**, *12*, 1884−1889.
(29) Envenson, S. A.; Fail, C. A.; Badyal, J. P. S *Chem. Mater.* **2000**, *12*, 3038−3043.
(30) Förch, R.; Zhang, Z.; Knoll, W. *Plasma Process. Polym.* **2005**, *2*, 351−372.
(31) Thierry, B.; Jasieniak, M.; de Smet, L. C. P. M; Vasilev, K.; Griesser, H. J. *Langmuir* **2008**, *24*, 10187−10195.
(32) Roth, J.; Albrecht, V.; Nitschke, M.; Bellmann, C.; Simon, F.; Zschoche, S.; Michel, S.; Luhmann, C.; Grundke, K.; Voit, B. *Langmuir* **2008**, *24*, 12603−1261.
(33) Friedrich, J.; Kühn, G.; Mix, R.; Unger, W. *Plasma Process. Polym.* **2004**, *1*, 28−50.
(34) Panousis, E.; Clément, F.; Loiseau, J.-F.; Spyrou, N.; Held, B.; Thomachot, M.; Marlin, L. *Plasma Sources Sci. Technol.* **2006**, *15*, 828−839.
(35) Lommatzsch, U.; Ihde, J. *Plasma Process. Polym.* **2008**, *6*, 642−648.
(36) Villermet, A.; Cocolios, P.; Rames-Laglande, G.; Coueret, F.; Gelot, J.-L.; Prinz, E.; Förster, F. *Surf. Coat. Technol.* **2003**, *174−175*, 899−901.
(37) Chen, Q.; Forch, R.; Knoll, W. *Chem. Mater.* **2004**, *16*, 614−620.
(38) Choukourov, A.; Biedermann, H.; Slavinska, D.; Hanley, L.; Grinevich, A.; Boldyryeva, H.; Mackova, A. *J. Phys. Chem. B* **2005**, *109*, 23086−23095.
(39) Gancarz, I.; Pozniak, G.; Bryjak, M.; Tylus, W. *Eur. Polym. J.* **2002**, *38*, 1937.
(40) Kim, J.; Shon, K.; Jung, D.; Moon, D. W.; Yun Han, D.; Geol Lee, T. *Anal. Chem.* **2005**, *77*, 4137−4141.
(41) Shard, A. G.; Whittle, J. D.; Beck, A. J.; Brookes, P. N.; Bullett, N. A.; Talib, R. A.; Mistry, A.; Barton, D.; McArthur, S. L. *J. Phys. Chem. B* **2004**, *108*, 12472−12480.
(42) Denis, L.; Cossement, D.; Godfroid, T.; Renaux, F.; Bittencourt, C.; Snyders, R.; Hecq, M. *Plasma Process. Polym.* **2009**, *6*, 199−208.

(43) Decher, G. *Science* **1997**, *277*, 1232−1236.
(44) Bergbreiter, D. E.; Boren, D.; Kippenberger, A. M. *Macromolecules* **2004**, *37*, 8686−8691.
(45) Tao, G. L.; Gong, A. J.; Lu, J. J.; Sue, H. J.; Bergbreiter, D. E. *Macromolecules* **2001**, *34*, 7672−7679.
(46) Girard-Lauriault, P. L.; Desjardins, P.; Unger, W. E. S.; Lippitz, A.; Wertheimer, M. R. *Plasma Process. Polym.* **2008**, *5*, 631−644.
(47) Nakamae, L.; Nishino, T.; Airu, X.; Asaoka, S. *Int. J. Adhesion Adhesives* **1995**, *15*, 15−20.
(48) Maguire, J. F.; Talley, P. L.; Lupkowski, M. *J. Adhes.* **1994**, *45*, 269−290.
(49) Bour, J.; Bardon, J.; Aubriet, H.; Del Frari, D.; Verheyde, B.; Dams, R.; Vangeneugden, D.; Ruch, D. *Plasma Process. Polym.* **2008**, *5*, 788−796.
(50) Gahsemi, M.; Minier, M.; Tatoulian, M.; Arefi-Khonsari, F. *Langmuir* **2007**, *23*, 11554−11561.
(51) Favia, P.; Stendardo, M. V.; D'agostino, R. *Plasmas Polym.* **1996**, *1*, 91−112.
(52) Charles, L. *Rapid Commun. Mass Spectrom.* **2008**, *22*, 151−155.
(53) DIN EN ISO 4624:2002 "*Pull-off test for adhesion*"
(54) Hegemann, D.; Hossain, M. M.; Körner, E.; Balazs, D. J. *Plasma Process. Polym.* **2007**, *4*, 229−238.
(55) Herbert, P. A. F.; O'Neill, L.; Jaroszynska-Wolinska, J. *Chem. Mater.* **2009**, *21*, 4401−4407.
(56) Bour, J.; Charles, L.; Petersen, J.; Michel, M.; Bardon, J.; Ruch, D. *Plasma Process. Polym.* **2010**, *7*, 687−694.
(57) Finke, B.; Schröder, K.; Ohl, A. *Plasma Process. Polym.* **2008**, *5*, 386−396.
(58) Yegen, E.; Zimmermann, U.; Unger, W. E. S.; Braun, T. *Plasma Process. Polym.* **2009**, *6*, 11−16.